Prefrontal Cortical Dysfunction After Overexpression Of Histone Deacetylase 1

Supplemental Information

Supplemental Methods

Analysis of Human Microarray Data

Two publicly accessible datasets were analyzed, the National Brain Databank: Brain Tissue Gene Expression Repository of Harvard Brain Tissue Resource Center and the Scripps Research Institute. The National Brain Databank utilized the Affymetrix HG-U133A gene chip. CHP files were obtained from the website (http://national_databank.mclean.harvard.edu/brainbank/Main) that had been generated using Affymetrix's MAS software. These include 25 normal control subjects, 19 with bipolar disorder, and 19 with schizophrenia. Demographic details have been previously published (1). The CHP log2 expression files were then merged using Affymetrix Expression Console Software with the annotation file and the annotated log2 results exported as a text file for third-party downstream analysis. The Scripps Research Institute utilized Human Genome U133 Plus 2.0 array. We reanalyzed this post mortem expression data obtained from the Gene Expression Omnibus (GEO accession GSE21138) based on diagnosis. The database includes 59 total subjects, 29 normal controls and 30 patients with schizophrenia. Demographic details have been previously published. Expression was converted from log2 expression to linear expression as fold average of normal controls. Diagnostic analyses were conducted using parametric tests for independent groups. One-way analysis of variance (ANOVA) with Dunnett's test for post-hoc comparison and independent *t*-tests were used for group comparisons. All *p*-values are two-tailed.

Animals

All animal experiments were approved by the Animal Use and Care Committee of the University of Massachusetts. C57BL/6J mice were obtained from Jackson Laboratories (Bar

Harbor, ME). Mice were held under specific pathogen-free conditions with food and water being supplied ad libitum in an animal facility with a reversed 12 h light/dark cycle (light off at 7:00 am) under constant conditions (21 ± 1°C; 60% humidity). All experiments were performed during the activity-phase of the mice (dark phase) with at least one day break between different tests. All experiments were performed at least three weeks after surgery.

Stereotactic delivery of AAV9 into the rostro-medial cortex: Mice were anesthetized with a ketamine/ xylazine cocktail (IP: 100 mg/kg, 15 mg/kg; Sigma Aldrich) and 1 µL of virus ($1x10^{10}$ genomic copies) was injected at a rate of 0.25 µL/min using a Hamilton syringe (Reno, NV), a micropump (Stoelting) and a stereotactic frame (Stoelting). Stereotactic coordinates were: +1.5 mm anterior/posterior; +/- 0.2 mm medial/lateral; -2 mm dorsal/ventral.

Antipsychotic Drug Treatment

For antipsychotic drug studies, adult male C57BL/6J mice, 10–15 weeks of age, were treated for 21 d with once daily intraperitoneal injections of saline or haloperidol (0.5 mg/kg) or clozapine (5 mg/kg) (Sigma, St. Louis, MO). Tissue (prefrontal cortex (PFC)) was harvested 60 min after the last treatment. Effects of anti-psychotic treatment were analyzed by one-way ANOVA with ‘treatment’ (saline vs. clozapine vs. haloperidol) as between group factors.

Behavioral Studies

T-Maze: This test was used to measure working memory performance (3, 4). The maze consisted of 3 equally sized arms (30 cm x 7.5 cm and 30 cm high) made from white plastic: one start-arm leading in a 90° angle to the two target arms (opposing each other). All arms were equipped with sliding doors. During the test mice were first confined in the start-arm. Once the door of this arm was opened the mouse was allowed to choose one of the target arms. The door of the opposing target-arm was closed until the mouse returned to the start arm. The protocol was repeated until the mouse had made 15 choices. To analyze the working memory

performance of a mouse we counted the alternations between the target arms and calculated the percentage of alternations in relation to the total number of possible alternations. Mice were tested on two consecutive days. Because this protocol measures spontaneous alternations, food deprivation in conjunction with baited arms was not used.

8-arm Radial Maze: This test measures working memory (5). The apparatus consisted of eight equally sized arms (57 cm long) extending from a circular platform. Mice were individually placed in the middle of the platform and allowed to freely explore the maze. The entries into the arms were recorded and the test was stopped when the mouse had entered all eight arms at least once. Reentries into already visited arms were counted as mistakes. The more 'mistakes' a mouse made, the worse the working memory performance was considered. Because this protocol basically measures spontaneous alternations, food deprivation in conjunction with baited arms was not used.

Open Field test measures locomotor activity in mice (6). The apparatus consisted of an arena (40 x 40 cm) surrounded by 40 cm high walls made from white plastic. The arena was illuminated with white light (350 lux). Mice were individually placed into the arena and allowed to explore the arena for 15 min. Total distance moved, indicative of locomotor activity, was tracked with the video-based EthoVision system (Noldus, Wageningen, The Netherlands).

Step-through Passive Avoidance test: To measure long-term memory we used a passive avoidance paradigm (7, 8). The experiments were performed in a two chamber passive avoidance box (Gemini, San Diego Instruments, San Diego, CA). Both boxes were equipped with a steel rod floor (20.5 x 25 cm surface) and interconnected by a sliding door. One box was illuminated by dim light (10 lux) and the other box was illuminated with bright white light (250 lux). Mice were started in the light compartment and were left there for 1 min, then the door, separating the two compartments, was opened and the latency to enter this dark compartment was determined. The door was closed and mice received a footshock (1 s, 0.25 mA) and thereafter were returned to their home cage. On the next day the same procedure was

repeated, with the difference that no footshock was delivered.

Novel Object Recognition test was used to measure long-term memory (9, 10). Mice were individually placed into an open field box (40 x 40 cm) surrounded by 40 cm high walls made from white plastic, illuminated with white light (350 lux) containing an object (light colored lid of a standard laboratory bottle, VWR) for 10 min. Twenty-four h later mice were placed into the same open field again for 10 min, with the difference that it contained an additional object (darker colored and differently shaped lid). Time spent at the object(s) was assessed for both days and the relative time spent at the new object on day 2 was calculated. Also, the time spent at the object on day 1 was used to determine novel object exploration (11).

Marble Burying is a test that measures repetitive/stereotyped behavior in rodents (12, 13). Macrolon cages (27 x 20.5 cm, 14.5 cm high) were filled with fresh corn crop bedding material up to a level of 4 cm. Six marbles were equally distributed in the cage and the mouse was placed into the cage for 30 min. Then the number of buried marbles was counted.

Vocalization (audible to the human ear) is present in adult mice and has been observed in laboratory mice in mildly to extremely stressful situations (14). Mice were grabbed by their tail and lifted from their cage and held 50 cm above the bench-top for 15 sec and then placed back into their cages. The occurrence (or no occurrence) of vocalization was noted and data from each treatment group is expressed as the proportion of mice that vocalized. Note that in adult mice, as opposed to pups and rats, ultrasonic vocalizations are not a sign of distress or communication of fear but important for mating behavior and social interactions (15).

Behavioral data (T-Maze, 8-arm Radial Maze, Step-through Passive Avoidance) were analyzed by two-way mixed ANOVA tests with ‘treatment’ (AAV-Hdac1 vs. AAV-LacZ) as between group factor and ‘day’ (of testing) as within group factor, followed by Newman-Keuls post-hoc comparisons and two-tailed unpaired *t*-tests. For other behavioral assays, two-tailed unpaired *t*-tests were applied. Differences from chance level of 50% (T-Maze and Novel Object Recognition tests) were determined with the Wilcoxon signed rank test.

ß-galactosidase Staining and Immunohistochemistry

Mice were perfused with 4% phosphate buffered formaldehyde. Brains were removed, postfixed in perfusion solution for 4 h and transferred to phosphate buffered sucrose solution (30%) and after two days frozen on dry ice (for X-Gal staining) or in -20°C cold 2-methyl butane (for immunohistochemistry). For enzyme histochemistry (X-gal stainings), brains were cut on a sliding microtome (Leica, Buffalo Grove, IL) and 25-µm-thick sections were processed as described previously (16). For immunohistochemistry, brains were cut on a cryostat (Leica, Wetzlar, Germany) for doublelabeling with anti-LacZ (Fitzgerald, Acton, MA) and (i) anti-NeuN (neuronal marker, Millipore, Schwalbach, Germany), (ii) the astrocytic marker S-100b, (iii) the oligo-dendrocytic marker CNPase (Sigma-Aldrich, Munich, Germany), or (iv) the microglial marker Iba-1 (Wako Chemicals, Neuss, Germany). The appropriate fluorescent secondary antibodies were used (Dianova, Hamburg, Germany).

Quantification of immunolabeled cells: cell counts were performed on an Axioskop microscope (Zeiss) equipped with a motorized stage and Neurolucida software-controlled computer system (Microbrightfield, Colchester, VT). Spaced serial 25-µm-thick sections (250 µm apart) were observed under low-power magnification (10× objective) with a 365/420-nm excitation/emission filter set (01, Zeiss, blue fluorescence). The nuclear staining allowed delineation of cortical structures using the Neurolucida software. Every 5th section of the cingulate cortex was analyzed per animal. The counting was performed under 40x objective. From every animal at least 6 sections were analyzed and on each section at least 100 LacZ+ cells were counted. Iba-1 positive microglia were counted using optical disector principle as described previously (17). Here, 3-4 sections per animal were analyzed.

Tissue Processing and Immunoblotting

The rostro-medial cortex was dissected using a mouse brain matrix for coronal sections (Braintree scientific, Braintree, MA). A 2 mm thick slice was cut between +1 mm to +3 mm from

the optic chiasm (corresponding to the same coordinates as seen from Bregma). Then this slice was further dissected using the corpus callosum (CC) as a landmark; one vertical cut for each hemisphere was made at the highest point of the CC, followed by one horizontal cut to remove the rest of the CC from the cortex tissue. All tissues were frozen immediately on dry ice and stored at -80°C.

Tissue samples for western blotting were homogenized in 300 µL of 0.025 M Tris-HCl (pH 7.5) supplemented with protease inhibitor (Roche, Indianapolis, IN) using a TissueRuptor (Qiagen, Valencia, CA). Then samples were supplemented with 5 x RIPA buffer (1% Triton X-100; 1% SDS) and rotated for 30 min at 4°C to ensure extraction of nuclear proteins. Lysates at 1 µg/µL protein concentration were denaturated in Laemmli buffer with beta-mercaptoethanol for 10 min at 100°C. Cell culture samples were directly denatured in Laemmli buffer under the same reducing conditions. Equal amounts of denaturated sample in a volume of 20 µL were electrophoretically separated on a 4%-20% Tris-HCl polyacrylamide gradient gel (Biorad, Hercules, CA) and blotted onto a nitrocellulose membrane (Biorad). The following primary antibodies were used: rabbit polyclonal anti HDAC1 (1:1000, Aviva Systems Biology, San Diego, CA), rabbit polyclonal anti acetylated Lysine (Ac-K2-100; Cell Signaling, Danvers, MA), mouse monoclonal anti NeuN (1:1500; Millipore, Billerica, MA), mouse monoclonal anti synapsin 1 (Synaptic Systems, Goettingen, Germany) and the modification independent rabbit polyclonal histone H3 (H3 pan, 1:50.000; Millipore) or mouse monoclonal anti ß-actin (1:5000; Sigma Aldrich, St. Louis, MO or Cell Signaling) were used as loading controls. Anti-rabbit or anti-mouse HRP-conjugated secondary antibodies (1:15000 or 1:5000, respectively, Sigma Aldrich, St. Louis, MO) in conjunction with chemiluminescence detection reagents (Thermo Scientific, Middletown, VA) and classical Biomax Films (Kodak, Rochester, NY) were used for visualization of the signal. When indicated, bands were densitometrically analyzed using the software Quantity One (Biorad). Normalized densities were calculated relative to the control.

Vector Cloning and Cell Culture Work

Mouse Hdac1 complementary DNA (cDNA) (Open Biosystems; clone id: 4976514) and pAAV-MCS (Adeno Associated Virus with Multiple Cloning Site; Stratagene, Santa Clara, CA) vectors were restriction digested with SalI and PspXI. The Hdac1 insert was ligated into the pAAV-backbone and size selected for successful ligation. For functional analysis the plasmid was transfected into mouse N1E-115 cells to test whether pAAV-MCS-Hdac1 leads to production of HDAC1 protein. After testing, the plasmid was packaged into the AAV9 capsid as described (16). Mouse N1E-115 neuroblastoma cells were grown in Dulbecco's Modified Eagle Medium (Invitrogen) containing 10% fetal bovine serum and 0.1% penicillin/streptomycin. One day before transfection cells were plated onto 6 well plates and the Medium was changed to the serum reduced Eagle´s Minimum Essential Medium (OpitMEM, Invitrogen) under omission of antibiotics. About 80% confluent cells (approximately 250.000 cells) were transfected with 4.0 µg of AAV-Hdac1 plasmid using Lipofectamine 2000. Controls were treated with Lipofectamine only. Cells were collected 24 h after transfection.

Mouse Microarray Studies

Total RNA was isolated from mouse cingulate cortex using the RNeasy Lipid Tissue kit (Qiagen). To remove remaining genomic DNA on column DNAseI treatment was performed. RNA integrity was assessed by Chip based capillary electrophoreses using the RNA 6000 Nano Chip on the Bioanalyzer (Agilent Techologies, Santa Clara, CA). Only samples with a RNA integrity number above 9 were included in the study and transcribed into single-stranded cDNA using the Ambion WT Expression Kit (life technologies, Grand Island, NY). Then samples were hybridized onto one GeneChip Mouse Gene 1.0 ST Array (Affymetrix, Santa Clara, CA), each, using a hybridization mix (100 mM MES, 1 M (Na+), 20 mM EDTA, 0.01% Tween-20; containing 1 µL of bovine serum albumin (50 mg/mL) and 1 µL of 10 mg/mL Herring Sperm DNA per 100 µL) for 16 h. Chips underwent multiple rounds of automated washing, were stained and finally

scanned with the Affymetrix GeneChip Scanner 3000 7G.

For analysis, the quality of microarray data was assessed employing the Bioconductor package, arrayQualityMetrics (18). Microarray data was then uploaded to MicroArray Computational Environment 2.0 (MACE), which employs Robust Multiarray Average to preprocess raw oligonucleotide microarray data. The preprocessed data were stored as base 2 log transformed real signal numbers and used for fold-change calculations and statistical tests. Mean signal values and standard deviations were first computed for each gene across samples and the fold-change of expression of a gene between treatment groups was calculated by taking the ratio of these mean signal values. To determine differential expression of genes MACE internally conducts a Student *t*-test with the expression signal values of the two hybridizations for all genes in the set.

Gene names were updated using the NCBI mouse gene database and the EMBL-EBI tool of the European Bioinformatics Institute. For the total of 317 genes that in the microarray experiment were changed by at least 1.2-fold in AAV-Hdac1 treated mice, we identified the human homologue for 80.13% of them, using EMBL-EBI tool of the European Bioinformatics Institute to compare mouse and human transcriptomes on the array. For genes for which no human homologue was readily available, Ensembl Genome Browser was used to determine predicted closest orthologs. The homologues are listed in **Table S1**.

Quantitative Reverse Transcriptase-Polymerase Chain Reaction (qRT-PCR)

RNA was transcribed into cDNA using Superscipt II or III (Invitrogen) and random hexamer primers. cDNA was thereafter run on a Applied Biosystems 7500 or Roche 2.0 light-cycler using the QuantiFast CYBR Green PCR kit (Qiagen). Primer pairs for Hdac1, Ttr, Cd74, H2-Aa, H2-Ab1, H2-Eb1, Npy and Gbp4 (**Table S2**) were designed using Primer Express or Primer 3 with the housekeeping transcript *Hprt (Hypoxanthine-guanine phosophoribosyltransferase*) as endogenous reference. Data analysis was performed using the

comparative $2^{-\Delta\Delta C(T)}$ method (19). For graphical presentation and statistical analysis, the mRNA level for each sample was expressed as percentage of the mean value of the control group. Because the qPCR data (AAV-Hdac1 versus AAV-LacZ mice) showed non-normal distribution (Kolmogorov–Smirnov) the non-parametric Mann-Whitney test was used to test for significance.

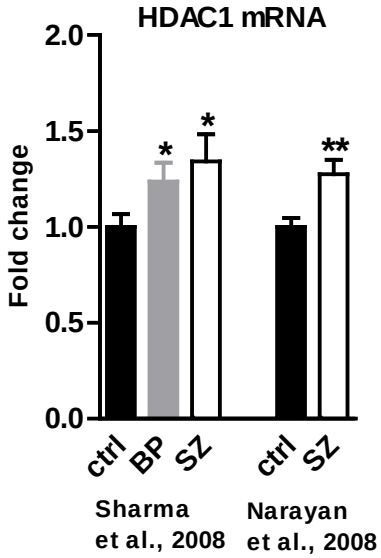

Figure S1. HDAC1 mRNA expression levels in human post mortem prefrontal cortex (PFC) of patients, diagnosed with bipolar disorder or schizophrenia. Fold changes of expression in two different cohorts: Harvard brain tissue resource center (left side of the bar graph) and Australian cohort (right side of the bar graph) in PFCs of control (ctrl; *n* = 25; 29; black bars), bipolar disorder (BP; *n* = 19; gray bar) and schizophrenia (SZ; *n* = 19; 30; white bars). Mean +/- SEM.

Figure S2. Coronal section at the rostralmost level of the hippocampus (H) of an AAV-LacZ injected animal, showing numerous labelled cells in hippocampal CA pyramidal layer and in medial cerebral cortex (CC). WM, white matter.

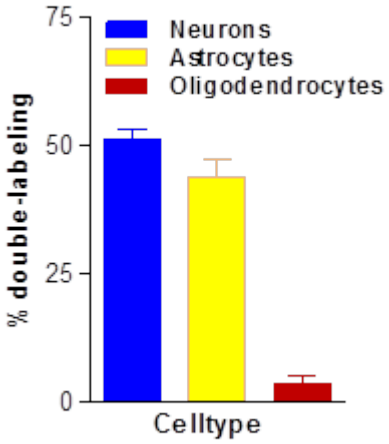

Figure S3. Quantification of AAV-LacZ transduced cells expressing immunoreactivity for the neuronal (NeuN, blue bar), the astrocytic (S100b, yellow bar) and the oligodendrocyte marker (CNPase, red bar).

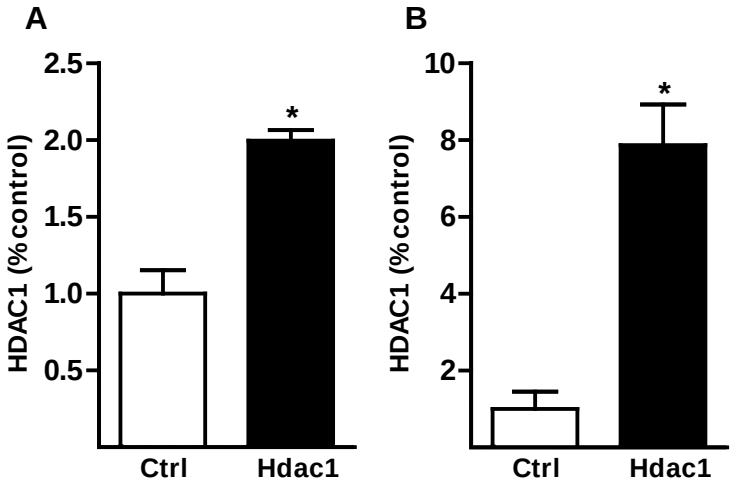

Figure S4. (**A, B**) Quantification of HDAC1 protein levels in (**A**) N1E-115 cells, non-transfected (white bar; *n* = 3) or transfected with the AAV-Hdac1 construct plasmid (black bar; *n* = 3) and (**B**) prefrontal cortex of mice injected with AAV-LacZ (white bar; *n* = 3) or AAV-Hdac1 (black bar; *n* = 3). ß-actin was used for a loading control. **p* < 0.05; *t*-tests.

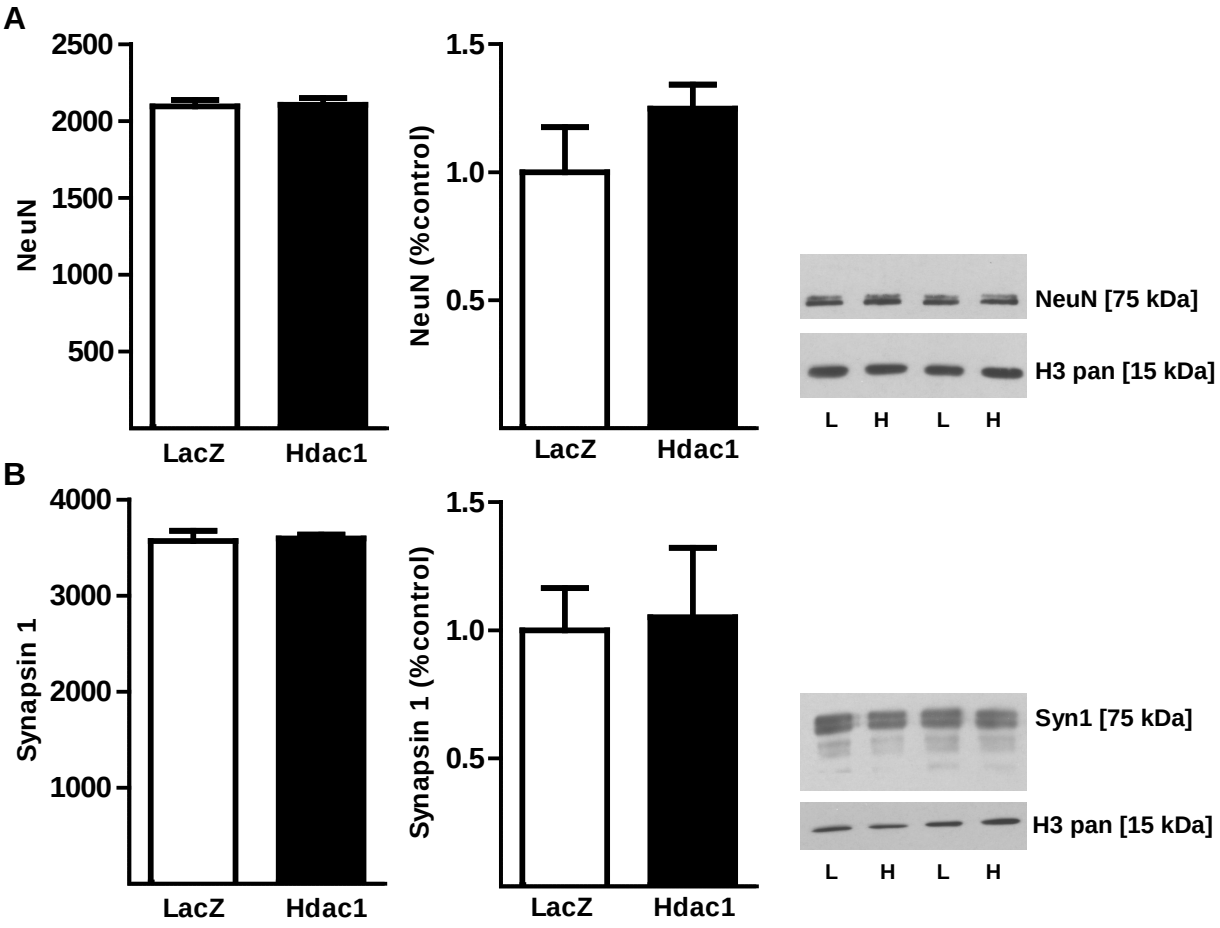

Figure S5. (**A**) Quantification of NeuN and (**B**) Synapsin 1 (Syn1) mRNA and protein levels in prefrontal cortex of mice injected with AAV-LacZ (white bars; *n* = 4) and AAV-Hdac1 (black bars; *n* = 4). Left bar graphs represent data derived from the microarray; right bar graphs show quantification of Western blot data normalized by the AAV-LacZ group. Right row: representative Western blots (L=AAV-LacZ; H=AAV-Hdac1). The modification independent Histone H3 (H3 pan) was used for a loading control.

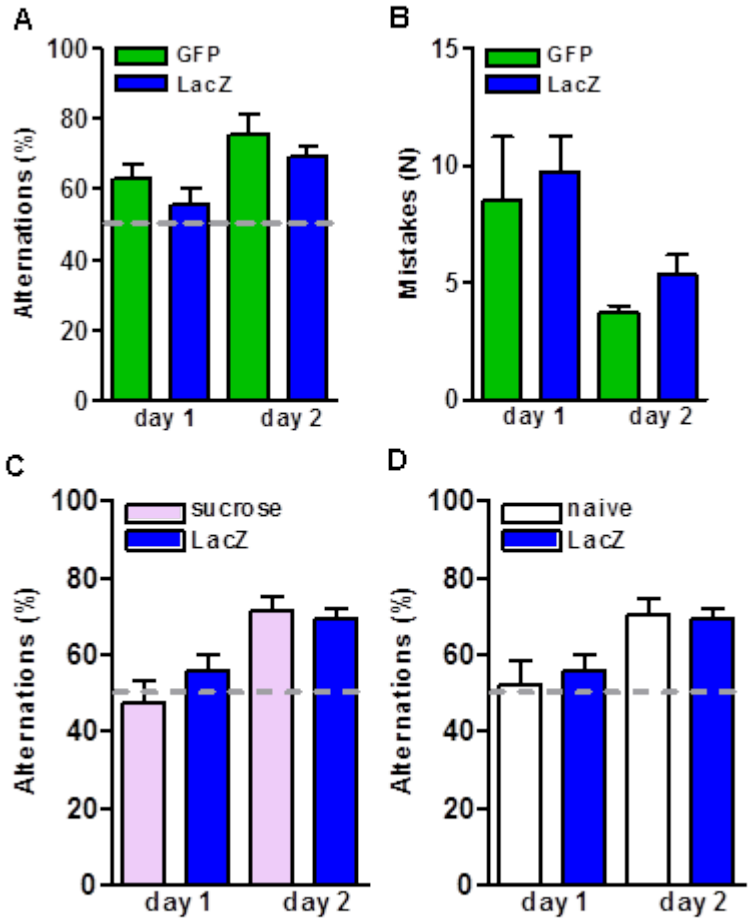

Figure S6. (**A, B**) Working memory in adult mice injected with AAV-GFP (green bars; *n* = 5) or AAV-LacZ (blue bars; *n* = 16) determined in (**A**) T-Maze or in (**B**) 8-arm Radial Maze. (**C, D**) Comparison of T-Maze performances of mice injected with AAV-LacZ (*n* = 16) with (**C**) mice injected with 5% sucrose (pink bars, *n* = 8) or (**D**) naive animals not exposed to surgery or any other procedure (white bars, *n* = 12). Notice normal working memory performances for each of the conditions and treatments.

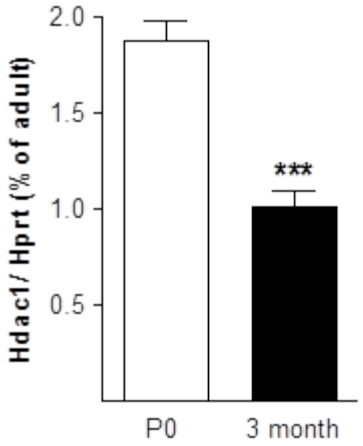

Figure S7. Hdac1 mRNA, normalized to Hprt mRNA, in newborn (P0) and adult prefrontal cortex.

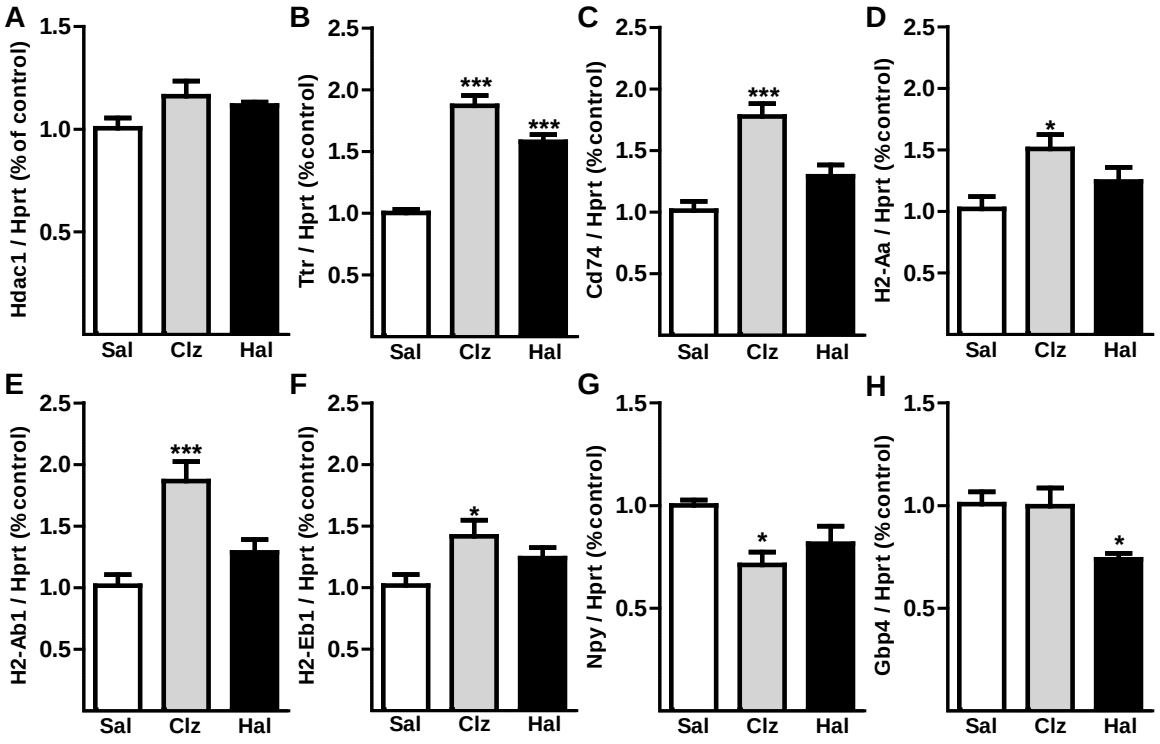

Figure S8. Gene expression changes after antipsychotic drug exposure in the prefrontal cortex. Bar graphs showing RNA levels for (**A**) Hdac1 ($F_{2,12}$ = 2.36, n.s.), (**B**) Ttr ($F_{2,12}$ = 52.25, p < 0.001), (**C**) Cd74 ($F_{2,12}$ = 17.81, p < 0.001), (**D**) H2-Aa ($F_{2,12}$ = 4.88, p < 0.05), (**E**) H2-Ab1 ($F_{2,12}$ = 12.66, p < 0.01), (**F**) H2-Eb1 ($F_{2,12}$ = 3.69, n.s.), (**G**) Npy ($F_{2,12}$ = 5.48, p < 0.05), and (**H**) Gbp4 ($F_{2,12}$ = 5.37, p < 0.05), following three weeks of daily systemic treatment with saline (Sal), clozapine (Clz) or haloperidol (Hal). Notice most pronounced effects on gene expression in Clz-treated animals. Data was normalized to *Hprt* housekeeping gene and calculated relative to the control (Sal) group. n = 5/group; * and *** p < 0.05 and p < 0.001 (Newman-Keuls following one-way ANOVA). Results of ANOVA are indicated behind each gene. n.s., not significant.

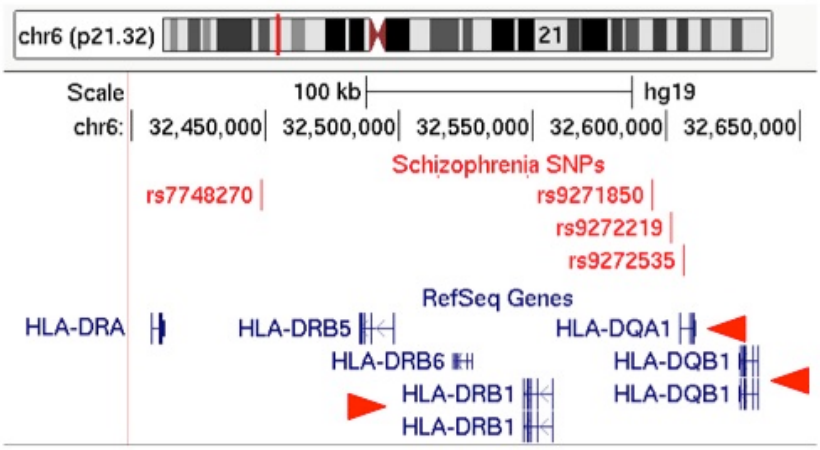

Figure S9. Browser window (200Kb) at schizophrenia risk locus on chr. 6p21.3-22.1, including position of single nucleotide polymorphisms (SNPs) associated with schizophrenia and bipolar disorder (see text). Arrowheads point to three *HLA* genes that were sensitive to Hdac1 exposure in the present study.

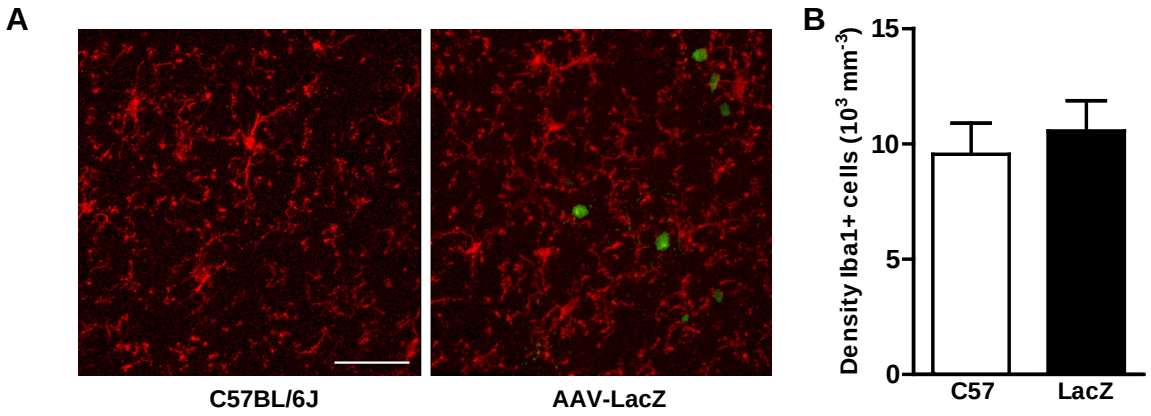

Figure S10. AAV injection does not affect the number of Iba-1 positive microglia in the prefrontal cortex. (**A**) Representative photomicrographs of untreated C57BL/6J mice, left side, and AAV9-LacZ injected C57BL/6J mice, right side. Green dots represent LacZ positive cells. Note the absence of overall increase in Iba-1 immunoreactivity in AAV-LacZ injected mice and particularly in proximity to the transduced cells. Scale bar: 30 µm. (**B**) Graph represents mean values + SEM for the stereologically estimated density of Iba-1 positive microglia in non-injected and injected cortex (*n* = 3/group).

Table S1. List of gene transcripts subject to >1.2 fold change in prefrontal cortex (PFC) of AAV-Hdac1 mice, compared to control, including fold-change (FC), *p*-value and false discovery rate (FDR). Human ID shows human homologues, light blue (yellow) = genes expressed at decreased (increased) levels ($p < 0.1$) in at least one of two schizophrenia cohorts (1, 2).

Note: decreased in diseased PFC; increased in diseased PFC

Downregulated Genes

Gene ID	FC	*p*-value	FDR	Human ID
ENSMUST00000103387 /// M28833 /// igkv4-1	-25.86	0.019	0.041	IGKV4-1
Ttr	-8.64	0.039	0.047	TTR
Cd74	-4.08	0.038	0.047	CD74
H2-Ab1	-3.84	0.025	0.044	HLA-DQB1
H2-Aa	-3.74	0.025	0.044	HLA-DQA1
Gbp4	-2.98	0.038	0.047	GBP4
Cxcl9	-2.23	0.047	0.049	CXCL9
Ighg	-2.23	0.028	0.045	IGHG
Gm12250 /// Ifi47 pseudogene	-2.18	0.036	0.047	
Irgm2 /// Igtp	-2.18	0.048	0.049	IRGC
LOC100046973	-2.08	0.048	0.049	
Serping1	-2.07	0.045	0.048	SERPING1
H2-Eb1	-2.07	0.028	0.045	HLA-DRB1
Ifi203	-1.99	0.047	0.049	IFI16
Gm7016 /// Ighv1-43	-1.85	0.043	0.048	
Art2b	-1.67	0.047	0.049	
Samhd1	-1.63	0.037	0.047	SAMHD1
Tmem140 /// 3110062M04Rik	-1.58	0.028	0.045	TMEM140
Igfbp7	-1.55	0.039	0.047	IGFBP7
Cp	-1.54	0.018	0.04	CP
Tnfsf10	-1.54	0.021	0.041	TNFSF10
Irf1	-1.52	0.044	0.048	IRF1
Ptpn22	-1.49	0.04	0.047	PTPN22
H2-DMa	-1.49	0.029	0.045	HLA-DMA
Tmem123	-1.48	0.039	0.047	TMEM123
Phxr4	-1.48	0.042	0.048	
Arhgdib	-1.48	0.037	0.047	ARHGDIB
C1s	-1.46	0.025	0.044	C1S
Gm5431	-1.46	0.044	0.048	
Gimap3	-1.45	0.018	0.04	GIMAP5
Psme2 /// Psme2b-ps	-1.44	0.045	0.048	PSME2
Stat4	-1.44	0.005	0.029	STAT4
Dcn	-1.44	0.025	0.044	DCN
2610301F02Rik /// ccdc141	-1.43	0.009	0.034	
AK134586 /// ENSMUST00000099760	-1.43	0.013	0.036	
Naaladl2	-1.41	0.005	0.029	
Irf4	-1.41	0.044	0.048	IRF4
Emcn	-1.4	0.04	0.047	EMCN
Havcr2	-1.4	0.05	0.05	HAVCR2
Cfh	-1.4	0.016	0.038	CFH
LOC100047860 /// Rpl21 pseudogene	-1.38	0.019	0.041	RPL21

Gene ID	FC	*p*-value	FDR	Human ID
Cd97	-1.37	0.009	0.034	CD97
Edem1	-1.36	0.027	0.045	EDEM1
Itga1	-1.36	0.01	0.034	ITGA1
Eltd1	-1.35	0.016	0.038	ELTD1
Prkcq	-1.35	0.038	0.047	PRKCQ
Tmem173	-1.35	0.044	0.048	TMEM173
Serpinb9	-1.35	0.001	0.021	SERPINB9
Slc22a8	-1.34	0.047	0.049	SLC22A8
Enpp1	-1.34	0.012	0.036	ENPP1
Gzmb	-1.33	0.043	0.048	GZMB
Cmpk2	-1.33	0.021	0.041	
Gvin1	-1.32	0.047	0.049	GVIN1
Entpd1	-1.32	0.046	0.049	ENTPD1
ENSMUST00000100430	-1.32	0.004	0.028	
Il10ra	-1.31	0.049	0.049	IL10RA
Abcb1b	-1.31	0.035	0.047	ABCB1
Slc16a6	-1.31	0.039	0.047	SLC16A6
Myd88	-1.3	0.027	0.045	MYD88
Bgn	-1.3	0.03	0.045	BGN
mmu-mir-505	-1.3	0.004	0.028	
Hhip	-1.3	0.048	0.049	HHIP
Cytip	-1.3	0.023	0.042	CYTIP
2610301F02Rik /// ccdc141	-1.3	0.015	0.038	
Tgfbi	-1.3	0.039	0.047	TGFBI
Abcb1a	-1.29	0.008	0.034	
Csmd3	-1.29	0.047	0.049	
chr16:6526419:6526726	-1.29	0.004	0.028	
Ifnar2	-1.29	0.038	0.047	IFNAR2
Aoah	-1.29	0.031	0.045	AOAH
Tbc1d7	-1.29	0.024	0.043	TBC1D7
Dgka	-1.29	< 0.001	< 0.001	DGKA
Vtn	-1.29	0.015	0.038	VTN
Fmod	-1.29	0.011	0.036	FMOD
Themis	-1.29	0.035	0.047	THEMIS
Pln	-1.29	0.004	0.028	PLN
Slc6a20a	-1.28	0.044	0.048	SLC6A20A
Cdh5	-1.28	0.016	0.038	CDH5
Edem2	-1.28	0.005	0.029	EDEM2
Larp1b	-1.28	0.016	0.038	LARP1B
Pcdhb18	-1.28	0.002	0.028	PCDHB18
Cysltr2	-1.28	0.021	0.041	CYSLTR2
GENSCAN00000024006	-1.28	0.05	0.05	
Heg1	-1.28	0.041	0.048	HEG1
Hibch	-1.28	0.009	0.034	HIBCH
Cnn2	-1.28	0.002	0.028	CNN2
Ammecr1	-1.27	0.022	0.042	AMMECR1
mmu-mir-100	-1.27	0.008	0.034	
Gm7482 /// Rps11 pseudogene	-1.27	0.028	0.045	RPS11P1
Iqgap1	-1.27	0.014	0.038	IQGAP1
Mrc1	-1.27	0.003	0.028	MRC1

Gene ID	FC	*p*-value	FDR	Human ID
Eng	-1.27	0.03	0.045	ENG
Gpr84	-1.27	0.027	0.045	GPR84
Il10rb	-1.27	0.032	0.046	IL10RB
5730522E02Rik	-1.27	0.021	0.041	
BC056474 /// Wdr83os	-1.26	0.017	0.04	
C5ar1	-1.26	0.042	0.048	C5AR1
Smc4	-1.26	0.023	0.042	SMC4
Rhoc	-1.26	0.032	0.046	RHOC
Itih5	-1.26	0.044	0.048	ITIH5
4632419I22Rik	-1.26	0.001	0.021	
Rras	-1.25	0.034	0.047	RRAS
Fxyd5	-1.25	0.026	0.045	FXYD5
Nfxl1	-1.25	0.007	0.034	NFXL1
Tmem43	-1.25	0.004	0.028	TMEM43
Tek	-1.25	0.042	0.048	TEK
Elf1	-1.25	0.042	0.048	ELF1
Creld2	-1.25	0.002	0.028	CRELD2
Hmcn1	-1.25	0.01	0.034	
Ptprb	-1.25	0.019	0.041	PTPRB
Ehd2	-1.24	0.004	0.028	EHDH2
Plod1 /// Myo5b	-1.24	0.031	0.045	PLOD1
4930420K17Rik	-1.24	0.04	0.047	C7orf23
Ehd4	-1.24	0.013	0.036	EHD4
Mccc1	-1.24	0.033	0.047	MCCC1
chr2:128606112:128606235	-1.24	0.027	0.045	
Gm10855	-1.24	0.007	0.034	
ENSMUST00000083840 /// U6	-1.24	0.023	0.042	
GENSCAN00000010976	-1.24	0.037	0.047	
Gbe1	-1.24	0.045	0.048	GBE1
Il6st	-1.24	0.042	0.048	IL6ST
Olfr804	-1.24	0.007	0.034	
Aim1	-1.24	0.045	0.048	AIM1
Gm7966// Nsa2-ps2	-1.23	0.021	0.041	
Itgb1	-1.23	0.011	0.036	ITGB1
Lcat	-1.23	0.004	0.028	LCAT
ENSMUST00000082570 /// U6	-1.23	0.021	0.041	
P2rx4	-1.23	0.01	0.034	P2RX4
Gm10484	-1.23	0.04	0.047	
Flt1	-1.23	0.015	0.038	FLT1
Slc6a13	-1.23	0.021	0.041	SLC6A13
ENSMUST00000082993 /// U1	-1.23	0.015	0.038	
Sclt1	-1.23	0.004	0.028	SCLT1
Cd2	-1.23	0.03	0.045	CD2
Fam111a	-1.23	0.004	0.028	FAM111A
AI747699 /// Lipo1	-1.23	0.018	0.04	
Il2ra	-1.23	0.012	0.036	IL2RA
Rbbp8	-1.23	0.003	0.028	RBBP8
Pnet-ps	-1.23	0.008	0.034	
AI324046 /// Ighg3	-1.23	0.049	0.049	
Txndc5	-1.23	0.001	0.021	TXNDC5

Gene ID	FC	*p*-value	FDR	Human ID
Zfp85-rs1	-1.23	0.008	0.034	
Serpinf1	-1.23	0.021	0.041	SERPINF1
Serpinb8	-1.23	0.001	0.021	SERPINB8
Tgfbr2 /// Mib1	-1.22	0.039	0.047	TGFBR2
Psmb10	-1.22	0.009	0.034	PSMB10
Oaz2	-1.22	0.009	0.034	OAZ2
9030420J04Rik /// Arhgap42	-1.22	0.013	0.036	
Slco1a4	-1.22	0.008	0.034	SLCO1A2
5830433M19Rik	-1.22	0.015	0.038	
Npy	-1.22	< 0.001	< 0.001	NPY
Lrrcc1	-1.22	0.002	0.028	LRRCC1
Arhgap29	-1.22	0.008	0.034	ARHGAP29
P2ry14	-1.22	0.04	0.047	P2RY14
Ms4a1	-1.22	0.021	0.041	MS4A1
Myl9	-1.22	0.023	0.042	MYL9
Kat2b	-1.22	0.031	0.045	KAT2B
4921513D11Rik	-1.22	0.038	0.047	
Rel	-1.22	0.008	0.034	REL
Myo1d	-1.22	0.048	0.049	MYO1D
Cflar	-1.22	0.011	0.036	CFLAR
Slc19a3	-1.22	0.003	0.028	SLC19A3
Hmcn1	-1.22	0.031	0.045	
Ifngr1	-1.22	0.048	0.049	IFNGR1
ENSMUST00000083152	-1.22	0.019	0.041	
Pls1	-1.21	0.015	0.038	PLS1
Magt1	-1.21	0.043	0.048	MAGT1
Egfl6	-1.21	0.036	0.047	EGFL6
ENSMUST00000083425 /// SNORD16	-1.21	0.011	0.036	
Klrc2	-1.21	0.031	0.045	KLRC2
P4ha3	-1.21	0.02	0.041	
6330406I15Rik	-1.21	0.021	0.041	C13orf33
Slc31a2	-1.21	0.018	0.04	
Gcnt1	-1.21	0.033	0.047	GCNT1
Snap23	-1.21	0.047	0.049	SNAP23
ENSMUST00000083890 /// 7SK	-1.21	0.006	0.031	
Gemin6	-1.21	0.036	0.047	GEMIN6
Galnt1	-1.21	0.005	0.029	GALNT1
Trmt112 /// Prdx5	-1.21	0.032	0.046	TRMT112
2810055G20Rik	-1.21	0.042	0.048	
Alg3	-1.21	0.047	0.049	ALG3
Pecam1	-1.21	0.032	0.046	PECAM1
Syne2	-1.21	0.009	0.034	SYNE2
1700020O03Rik	-1.21	0.001	0.021	C14orf118
Btd	-1.21	0.016	0.038	BTD
Tlr11	-1.21	0.009	0.034	
Rapgef6	-1.21	0.01	0.034	RAPGEF6
Adap2	-1.21	0.048	0.049	ADAP2
5830472F04Rik	-1.21	0.034	0.047	
FM991906 /// D81 snoRNA	-1.21	0.01	0.034	
Isyna1	-1.2	0.021	0.041	ISYNA1

Gene ID	FC	*p*-value	FDR	Human ID
Foxf1a	-1.2	0.036	0.047	FOXF1
Gabpb1	-1.2	0.014	0.038	GABPB1
Anxa1	-1.2	0.037	0.047	ANXA1
5033414D02Rik /// Plg-R(KT)	-1.2	0.003	0.028	
Dpp4	-1.2	0.018	0.04	DPP4
Nudt12	-1.2	0.036	0.047	NUDT12
Cyp1b1 /// 1700038P13Rik	-1.2	0.042	0.048	CYP1B1
7120432I05Rik	-1.2	0.023	0.042	
0610007P08Rik /// Sr278	-1.2	0.021	0.041	
Hmcn1	-1.2	0.015	0.038	
Dnm3os	-1.2	0.046	0.049	DNM3OS
Ascc3	-1.2	< 0.001	0.021	ASCC3

Upregulated Genes

Gene ID	FC	*p*-value	FDR	Human ID
Gm4864 /// Hdac1 pseudogene	10.87	< 0.001	< 0.001	HDAC1
ENSMUST00000097231 /// SNORD115	1.57	0.003	0.028	
ENSMUST00000099414 /// zfp955b	1.51	0.038	0.047	
ENSMUST00000101951 /// SNORD115	1.50	0.003	0.028	
Rny1	1.48	0.005	0.029	
NC_005089 /// mtDNA	1.47	0.007	0.034	
ENSMUST00000075293 /// Ppia pseudogene	1.47	0.027	0.045	
ENSMUST00000101803 /// SNORD115	1.39	0.012	0.036	
Olfr767	1.39	0.014	0.038	
ENSMUST00000101941 /// SNORD115	1.35	0.012	0.036	
Hamp2	1.34	0.037	0.047	HDAMP
Fcrls	1.34	0.047	0.049	
Gm9568	1.34	0.038	0.047	
Snord49b	1.34	0.036	0.047	
Ngp	1.33	0.011	0.036	
ENSMUST00000101879 /// SNORD 115	1.33	0.008	0.034	
Olfr763	1.32	0.034	0.047	
Gm5841 /// usp1 pseudogene	1.30	0.038	0.047	
chr14:32267718:32267807	1.30	< 0.001	< 0.001	
ENSMUST00000083173 /// n-R5s88	1.29	0.012	0.036	
Olfr64	1.29	0.001	0.021	
Dnajb6	1.29	0.025	0.044	DNAJB6
Krtap4-7	1.29	0.028	0.045	
2610206C17Rik	1.28	0.018	0.04	
Olfr672	1.28	0.002	0.028	
Btnl5	1.28	0.012	0.036	
ENSMUST00000082772 /// Y RNA	1.28	0.003	0.028	
chr10:77197596:77197890	1.28	0.011	0.036	
ENSMUST00000118182 /// Gapdh pseudogene	1.27	0.005	0.029	GAPDH
ENSMUST00000101908 /// SNORD115	1.27	0.031	0.045	
ENSMUST00000101944 /// SNORD115	1.27	0.003	0.028	
BC086805	1.27	0.002	0.028	
Gulo	1.27	0.006	0.031	
Pabpn1l	1.26	0.005	0.029	
Olfr850	1.26	0.031	0.045	

Gene ID	FC	*p*-value	FDR	Human ID
V1rd22	1.26	0.033	0.047	
Snhg1	1.26	0.018	0.04	SNHG1
3110053B16Rik /// Hpcal1 pseudogene	1.26	0.023	0.042	HPCAL1
Cntd1 /// Becn1	1.26	0.012	0.036	CNTD1
Olfr517	1.25	0.035	0.047	
GENSCAN00000028249	1.25	0.003	0.028	
Olfr1193	1.25	0.005	0.029	
AK081116	1.25	0.009	0.034	
Gm5064 /// Csde1 pseudogene	1.25	0.04	0.047	CSDE1
AJ311366 /// ENSMUST00000103569 /// Trav3-1	1.25	0.043	0.048	
Il23a	1.25	0.023	0.042	IL23A
Olfr985	1.24	0.022	0.042	
ENSMUSG00000073810 /// Ifnz	1.24	0.031	0.045	
Cela3b	1.24	0.015	0.038	CELA3B
chr4:138383291:138383391	1.24	0.003	0.028	
ENSMUST00000119302 /// Kif22 pseudogene	1.24	0.004	0.028	KIF22
Gm52 /// Syna	1.24	0.001	0.021	
Gm10815	1.24	0.013	0.036	
Accsl	1.24	0.028	0.045	
Stfa2	1.24	0.031	0.045	CSTA
Gm7673 /// Vmn1r224	1.24	0.017	0.04	
Olfr97	1.24	0.044	0.048	
Fer1l6	1.24	0.006	0.031	
Gpihbp1	1.24	0.009	0.034	GPIHBP1
3110018I06Rik	1.24	0.022	0.042	
Olfr765	1.24	0.026	0.045	
Rangrf /// Slc25a35	1.24	0.048	0.049	RANGRF
Lcn8	1.23	0.036	0.047	LCN8
Olfr367	1.23	0.03	0.045	
V1re1	1.23	0.04	0.047	
LOC674866 /// similar to Gapdh	1.23	0.004	0.028	
Gm10785	1.23	0.019	0.041	
Gm8598 /// Cox11 pseudogene	1.23	0.009	0.034	
Olfr225	1.23	0.008	0.034	
Serpinb3c	1.23	0.034	0.047	SERPINB3
Gm379 /// Stx3 pseudogene	1.22	0.02	0.041	
ENSMUST00000101925 /// n-R5s1	1.22	0.012	0.036	
Gm5121	1.22	0.013	0.036	
7420426K07Rik	1.22	0.005	0.029	
BC048562	1.22	0.001	0.021	
Olfr640	1.22	0.025	0.044	OR51I1
Dppa3	1.22	0.013	0.036	
Olfr1297	1.22	0.045	0.048	
A430072C10Rik /// Q8C9Y9	1.22	0.031	0.045	
Olfr1428	1.22	0.039	0.047	
AY026312 /// Krtap16-10b	1.22	0.028	0.045	
Olfr101	1.22	0.031	0.045	OR12D2
Myh6 /// Myh7	1.22	0.013	0.036	MYH6
Osr2	1.22	0.016	0.038	OSR2
Gm5666 /// Hmgb3 pseudogene	1.22	0.005	0.029	HMGB3

Gene ID	FC	*p*-value	FDR	Human ID
Gm8681 /// Hmgb2 pseudogene	1.22	0.019	0.041	HMGB2
GENSCAN00000039359	1.22	0.012	0.036	
ENSMUST00000083801 /// SNORD77	1.22	0.029	0.045	
Selp	1.22	0.001	0.021	SELP
Trdn	1.22	0.041	0.048	TRDN
ENSMUST00000118391 /// Fthl17 pseudogene	1.21	0.039	0.047	
Olfr149	1.21	0.021	0.041	
1700034J05Rik	1.21	0.01	0.034	
Vmn2r56	1.21	0.022	0.042	
Cyp4a14	1.21	0.039	0.047	CYP4A22
Asb10	1.21	0.01	0.034	ASB10
Cfi	1.21	0.037	0.047	CFI
chr4:153570616:153570666	1.21	0.027	0.045	
Olfr134	1.21	0.006	0.031	
mmu-mir-320	1.21	0.004	0.028	
Mcpt4	1.21	0.001	0.021	
Cyp2d40	1.21	0.042	0.048	CYP2D6
Gm8824 /// Gaph pseudogene	1.21	0.029	0.045	
Olfr1370	1.21	0.024	0.043	
chr1:49635994:49636346	1.21	0.006	0.031	
Gm8055 // Gapdh pseudogene	1.21	0.004	0.028	
Srpx /// Rpgr	1.20	0.021	0.041	SRPX
ENSMUST00000083134 /// n-R5s5	1.20	0.044	0.048	
GENSCAN00000008377	1.20	0.029	0.045	
Amigo3	1.20	0.003	0.028	AMIGO3
ENSMUST00000083772 /// SNORA61	1.20	0.01	0.034	
ENSMUST00000083937	1.20	0.006	0.031	
Gpx2	1.20	0.031	0.045	GPX2
D130052B06Rik	1.20	0.014	0.038	

Table S2. PCR primer sequences (mouse RNA), including gene ID and product size.

Gene symbol	Gene ID #	Primer sequence		Product size
		forward	*reverse*	
Hdac1	NM_008228.2	**TCC AGC AGC GAG CAA CAT T**	**CAA AGG ACA CGC CAA GTG TGT**	104 bp
Hdac1	NM_008228.2	**AAA GGA CAC GCC AAG TGT GTG**	**TGT TTC GTA AGT CCA GCA GCG**	114 bp
Hprt	NM_013556.2	**GTT CTT TGC TGA CCT GCT GGA**	**TCC CCC GTT GAC TGA TCA TT**	120 bp
Ttr	NM_013697.5	**TGC TGG AGA ATC CAA ATG TC**	**GAA ATG CCA AGT GTC TTC CA**	243 bp
Cd74	NM_010545.3	**GAA CCT GCA ACT GGA GAG CC**	**GGT TTG GCA GAT TTC GGA AG**	51 bp
H2-Aa	NM_010378.2	**CAT TCA AGG CCT GCG ATC A**	**TCA CCC AGC ACA CCA CTT CTT**	113 bp
H2-Ab1	NM_207105.3	**GAA CAG CCC AAT GTC GTC ATC**	**GGA ACC AGC GCA CTT TGA TCT**	115 bp
H2-Eb1	NM_010382.2	**CCT GAT GGC TGT TTA TCC CTG**	**TGA CAG CAG ACT GGC TCA GAA**	125 bp
Npy	NM_023456.2	**CCG CTC TGC GAC ACT ACA T**	**TGT CTC AGG GCT GGA TCT CT**	68 bp
Gbp4	NM_001256005.1	**TGT CAG TGA ACC AGG AAG CC**	**GAA ACC TTT GGC TGG TAG GC**	162 bp

Table S3. Results of Two-way mixed ANOVAs on behavioral tests.

	Genotype		Day		Genotype X Day	
	F	***p***	***F***	***p***	***F***	***p***
T-maze $_{(1,36)}$	7.62	0.01	6.24	0.05	1.88	n.s.
Radial Maze $_{(1,22 \text{ and } 3,66)}$	8.87	0.01	3.17	0.05	0.32	n.s.
Passive Avoidance $_{(1,26)}$	0.22	n.s.	30.86	0.001	1.67	n.s.

The degrees of freedom for F are indicated in brackets.
n.s., not significant.

Supplemental References

1. Sharma RP, Grayson DR, Gavin DP (2008): Histone deactylase 1 expression is increased in the prefrontal cortex of schizophrenia subjects: analysis of the National Brain Databank microarray collection. *Schizophr Res*. 98:111-117.

2. Narayan S, Tang B, Head SR, Gilmartin TJ, Sutcliffe JG, Dean B, *et al.* (2008): Molecular profiles of schizophrenia in the CNS at different stages of illness. *Brain Res.* 1239:235-248.

3. Brito LS, Yamasaki EN, Paumgartten FJ, Brito GN (1987): Continuous and discrete T-maze alternation in rats: effects of intertrial and interrun intervals. *Braz J Med Biol Res.* 20:125-135.

4. Deacon RM, Rawlins JN (2006): T-maze alternation in the rodent. *Nat Protoc.* 1:7-12.

5. Kolata S, Wu J, Light K, Schachner M, Matzel LD (2008): Impaired working memory duration but normal learning abilities found in mice that are conditionally deficient in the close homolog of L1. *J Neurosci.* 28:13505-13510.

6. Ramos A, Mormede P (1998): Stress and emotionality: a multidimensional and genetic approach. *Neurosci Biobehav Rev.* 22:33-57.

7. Davis HP, Spanis CW, Squire LR (1976): Inhibition of cerebral protein synthesis: performance at different times after passive avoidance training. *Pharmacol Biochem Behav.* 4:13-16.

8. Morellini F, Sivukhina E, Stoenica L, Oulianova E, Bukalo O, Jakovcevski I, *et al.* (2010): Improved reversal learning and working memory and enhanced reactivity to novelty in mice with enhanced GABAergic innervation in the dentate gyrus. *Cereb Cortex.* 20:2712-2727.

9. Clarke JR, Cammarota M, Gruart A, Izquierdo I, Delgado-Garcia JM (2010): Plastic modifications induced by object recognition memory processing. *Proc Natl Acad Sci U S A.* 107:2652-2657.

10. Weible AP, Rowland DC, Monaghan CK, Wolfgang NT, Kentros CG (2012): Neural correlates of long-term object memory in the mouse anterior cingulate cortex. *J Neurosci.* 32:5598-5608.

11. Powell SB, Paulus MP, Hartman DS, Godel T, Geyer MA (2003): RO-10-5824 is a selective dopamine D4 receptor agonist that increases novel object exploration in C57 mice. *Neuropharmacology*. 44:473-481.

12. Takeuchi H, Yatsugi S, Yamaguchi T (2002): Effect of YM992, a novel antidepressant with selective serotonin re-uptake inhibitory and 5-HT 2A receptor antagonistic activity, on a marble-burying behavior test as an obsessive-compulsive disorder model. *Jpn J Pharmacol.* 90:197-200.

13. Malkova NV, Yu CZ, Hsiao EY, Moore MJ, Patterson PH (2012): Maternal immune

activation yields offspring displaying mouse versions of the three core symptoms of autism. *Brain Behav Immun.* 26:607-616.

14. Whitney GD (1969): Vocalization of mice: a single genetic unit effect. *J Heredity.* 60:337-340.

15. Portfors CV (2007): Types and functions of ultrasonic vocalizations in laboratory rats and mice. *JAALAS.* 46:28-34.

16. Jakovcevski M, Guo Y, Su Q, Gao G, Akbarian S (2010): rAAV9--a human-derived adeno-associated virus vector for efficient transgene expression in mouse cingulate cortex. *Cold Spring Harb Protoc*. 2010:pdb prot5417.

17. Schmid JS, Bernreuther C, Nikonenko AG, Ling Z, Mies G, Hossmann KA, *et al.* (2012): Heterozygosity for the mutated X-chromosome-linked L1 cell adhesion molecule gene leads to increased numbers of neurons and enhanced metabolism in the forebrain of female carrier mice. *Brain Struct Funct*. [epub ahead of print].

18. Kauffmann A, Gentleman R, Huber W (2009): arrayQualityMetrics--a bioconductor package for quality assessment of microarray data. *Bioinformatics*. 25:415-416.

19. Livak KJ, Schmittgen TD (2001): Analysis of relative gene expression data using real-time quantitative PCR and the 2(-Delta Delta C(T)) Method. *Methods.* 25:402-408.